

## Bandgap engineering of Cd<sub>x</sub>Zn<sub>1-x</sub>Te nanowires†

Cite this: *Nanoscale*, 2013, 5, 932

Keivan Davami,<sup>a</sup> Judith Pohl,<sup>‡b</sup> Mehrdad Shaygan,<sup>‡a</sup> Nazli Kheirabi,<sup>‡a</sup> Hamid Faryabi,<sup>a</sup> Gianaurelio Cuniberti,<sup>b</sup> Jeong-Soo Lee<sup>\*a</sup> and M. Meyyappan<sup>\*c</sup>

Received 22nd October 2012

Accepted 17th December 2012

DOI: 10.1039/c2nr33284a

www.rsc.org/nanoscale

Bandgap engineering of single-crystalline alloy Cd<sub>x</sub>Zn<sub>1-x</sub>Te (0 ≤ x ≤ 1) nanowires is achieved successfully through control of growth temperature and a two zone source system in a vapor–liquid–solid process. Extensive characterization using electron microscopy, Raman spectroscopy and photoluminescence shows highly crystalline alloy nanowires with precise tuning of the bandgap. It is well known that bulk Cd<sub>x</sub>Zn<sub>1-x</sub>Te is popular for construction of radiation detectors and availability of a nanowire form of this material would help to improve detection sensitivity and miniaturization. This is a step forward towards the accomplishment of tunable and predetermined bandgap emissions for various applications.

### 1 Introduction

One-dimensional nanostructures have been explored for nanoscale devices such as lasers, waveguides, and optical switches,<sup>1</sup> all of which require a wide variety of energy gaps. Since common semiconductors have a fixed bandgap in a limited range, new methods are sought for bandgap modulation. Heterostructure nanowires have been an early solution with the heterointerface either parallel to the axis called a radial junction or perpendicular to the axis called an axial junction. These structures have been used in solar cells<sup>2,3</sup> and field effect transistors.<sup>4</sup> Alloy nanowires as a second method<sup>5–12</sup> show the ability to tune the bandgaps, but it is far from maturity needed for routine device fabrication. Alloy nanowires in various systems have been used to construct solar cells, photodetectors, nanoscale lasers and light emitting diodes.<sup>9</sup>

CdTe and ZnTe with bandgaps of 1.44 eV and 2.26 eV respectively at 300 K show interesting properties in infrared and visible regions. High quality ZnTe and CdTe nanowires have been grown using the vapor–liquid–solid (VLS) method in recent years due to their potential applications in thermoelectric devices.<sup>13,14</sup> It is well known that the alloy of Cd and Zn tellurides in the bulk form, known as CZT, is highly desirable for radiation detection.<sup>15,16</sup> The wide bandgap of CZT enables room temperature operation of radiation detectors. The inherent high resistivity of CZT allows low leakage currents and noise levels compared to pure CdTe detectors.<sup>16</sup> It is desirable to develop CZT nanowires due to the possibility to increase the detection sensitivity and potential for miniaturization. Here we report catalytic growth and thorough characterization of Cd<sub>x</sub>Zn<sub>1-x</sub>Te (0 ≤ x ≤ 1) nanowires. Highly crystalline nanowires without any crystal defects have been obtained. Continuous tuning of x from zero to one was achieved by precise control of the substrate temperature and precursors, and the subsequent tuning of the bandgap of Cd<sub>x</sub>Zn<sub>1-x</sub>Te nanowires allows emission from green (528 nm) to infrared (855 nm) region.

### 2 Experimental procedure

#### Growth method

A VLS technique was used for the growth of the alloy nanowires. Thermally oxidized silicon substrates with a 100 nm thick oxide layer and 3 nm thin gold layer were placed in the downstream heating zone of a quartz tube (diameter of 2.54 cm) inserted into a furnace. In a set of trial experiments, ZnTe (99.99% Aldrich) and CdTe (99.99% Aldrich) source powders were mixed together in different ratios (1 : 1, 1 : 5, 5 : 1, 2 : 5, 5 : 2) in a quartz boat. The source zone was heated to 700 °C while two different substrate temperatures were examined at 420 °C and 500 °C. The temperature was ramped at a rate of 15 °C min<sup>-1</sup>, after purging the tube using nitrogen three times. A carrier gas mixture of 10 sccm argon and 5 sccm hydrogen was used at a pressure of 1.4 × 10<sup>-1</sup> Torr. After a growth period of 1 hour, the substrates inside the quartz tube were cooled down to room

<sup>a</sup>Division of IT Convergence Engineering, Pohang University of Science and Technology, Pohang, Republic of Korea. E-mail: ljs6951@postech.ac.kr

<sup>b</sup>Technical University of Dresden, Dresden, Germany

<sup>c</sup>NASA Ames Research Center, Moffett Field, CA 94035, USA. E-mail: m.meyyappan@nasa.gov

† Electronic supplementary information (ESI) available: Alloy nanowire growth and characterization. See DOI: 10.1039/c2nr33284a

‡ These authors contributed equally.

temperature under vacuum before removal. Regardless of the ratio of CdTe and ZnTe or the substrate temperature, the resulting nanowires from these trials contained only  $\sim 5.0\%$  Cd. The use of individual boats of CdTe and ZnTe sources did not result in controllable CZT composition either. Therefore, a second set of runs was performed using a novel approach; considering the difference between the vapor pressures of CdTe and ZnTe, in addition to the first boat of CdTe mixed with ZnTe at a ratio of 1 : 1, another boat of CdTe was placed in the middle of the furnace. The temperature of the source material increased to  $700\text{ }^\circ\text{C}$  at the location of the first boat and due to the temperature gradient inside the tube, the temperature in the vicinity of the second boat was measured to be  $\sim 650\text{ }^\circ\text{C}$ . Different substrate temperatures were used ( $360\text{ }^\circ\text{C}$ ,  $380\text{ }^\circ\text{C}$ ,  $400\text{ }^\circ\text{C}$ ,  $420\text{ }^\circ\text{C}$ ,  $450\text{ }^\circ\text{C}$ ,  $470\text{ }^\circ\text{C}$ , and  $500\text{ }^\circ\text{C}$ ) and the results were compared to confirm successful control of alloy composition.

### Characterization

The surface morphology of the nanowires was investigated using a field emission scanning electron microscope (SEM) (JEOL JSM-7401F) operated at 5 kV. A high resolution transmission electron microscope HR-TEM (JEOL JEM-2100F with Cs Corrected on STEM) operated at 200 kV was used to study the crystalline structures of the as-grown nanowires. The TEM was equipped with an energy dispersive X-ray spectrometer (EDX) which was used to evaluate the composition of the nanowires. Raman spectroscopy analysis was done in a Senterra Raman spectroscope (Bruker Optics), using the excitation wavelength of 532 nm from a Nd:YAG laser. The spot size of the laser was 500 nm and an optical microscope was used to choose the probing area. The laser power for all the samples except CdTe nanowires was 0.2 mW, selected to prevent damaging of the nanowires due to local heating effects; the power for CdTe nanowires was 10 mW. The integration time was 100 s and no particular sample preparation was used for the analysis.

The structural characterization of the samples was carried out by an X-ray diffractometer (D/Max-2500/PC made by Raigaku Co.), using Cu-K $\alpha$  ( $\lambda = 1.5418\text{ \AA}$ ) radiation at 100 mA, 40 keV. The XRD patterns were recorded in the scanning angle range of  $5\text{--}90^\circ$  with a scanning speed of  $4^\circ$  per min. In order to interpret the pattern and identify the observed peaks, the Joint Committee of Powder Diffraction Standard (JCPDS) card file data were used. The standard diffraction patterns of CdTe (JCPDS card no. 15-0770) and ZnTe (JCPDS card no. 15-0746) were assigned as references. The PL measurement was carried out at room temperature using an Alpha300 Raman spectrometer system (WITec, Ulm, Germany). The system was equipped with a 532 nm and a 785 nm laser source. For the measurements here, the 532 nm diode laser with a spot size of 500 nm and 1 mW excitation power was focused on the sample at a microscope scanning stage through a  $100\times$  objective (Nikon, Melville, NY, USA).

## 3 Results and discussion

As mentioned above, accounting for the difference in the vapor pressures of the two materials through this approach then

allowed control of alloy composition by simply varying the substrate temperature between  $360$  and  $500\text{ }^\circ\text{C}$  as seen in Fig. 1a. The Cd fraction increases with a decrease in substrate temperature and no nanowires were formed at temperatures lower than  $360\text{ }^\circ\text{C}$ . In all cases, a powder-like coating covered the surface of the substrates and the color of the coating varied from reddish-brown (similar to ZnTe source powder color) to gray (the color of CdTe source powder). The diameter of the nanowires is in the range of 50 nm to 150 nm and their lengths are around several tens of micrometers. The nanowires are largely cylindrical though some tapered structures were observed at temperatures lower than  $420\text{ }^\circ\text{C}$ .

A comprehensive characterization of several as-grown nanowires at different temperatures was conducted. HRTEM and diffraction patterns (Fig. S1, ESI $^\dagger$ ) illustrate that the growth direction along the whole length of the nanowire is (111). As can be seen in the EDX results (Fig. S1(c), ESI $^\dagger$ ), the difference in the Cd amount in the beginning and end of the nanowire is negligible, which was recorded for several nanowires. This uniformity is attributed to the source distribution mentioned earlier. The lowest ratio obtained for the Cd amount between the two ends of a nanowire was  $\sim 0.80$ . In contrast, nanowires with similar dimensions grown with two individual boats of CdTe and ZnTe powders exhibited a Cd ratio (beginning to end) of  $\sim 1.7$ .<sup>17</sup> Te aggregation was not observed in any of the samples, which indicates the proper alloying of Zn, Cd, and Te in our nanowires. Crystal defects such as stacking faults and twins common in the catalytically grown nanowires were not observed

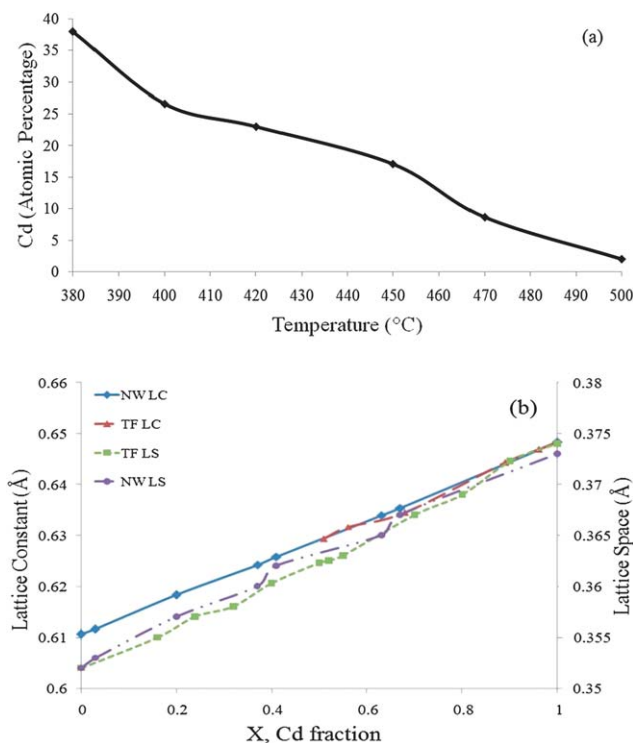


**Fig. 1** (a) Cd atomic percentage versus temperature, (b) lattice spacing and lattice constant versus Cd composition. LC and LS are lattice constant and lattice spacing respectively. NW denotes the data for nanowires from this work. TF denotes data for thin films from ref. 18 and 19.

in any of the HRTEM images and diffraction patterns. Indeed, alloying ZnTe nanowires with Cd has recently been suggested as a method to reduce the crystal defects in nanowires.<sup>17</sup> This was attributed to the reduction of the interfacial instability during the growth process *via* minimizing the surface energy which causes the formation of uniform zincblende crystals instead of a combination of zincblende–wurtzite structures.<sup>17</sup> The XRD patterns of nanowires with different compositions here (Fig. S2, ESI†) confirm the crystalline structure of  $\text{Cd}_x\text{Zn}_{1-x}\text{Te}$  without any other phases or impurities. The crystal structure of  $\text{Cd}_x\text{Zn}_{1-x}\text{Te}$  is determined as zincblende throughout the whole range of compositions by the presence of (111), (220), and (311) peaks in the XRD patterns. With an increase in the Cd fraction in the alloy, the peaks shift towards the peaks of CdTe.

The lattice spacing for different compositions was calculated based on the XRD results and the estimation of nanowire lattice constants ( $\alpha$ ) for preferentially oriented (111) reflection from the XRD pattern using the formula:  $\alpha = d\sqrt{(h^2 + k^2 + l^2)}$  where  $\alpha$  is the lattice constant,  $d$  is the lattice spacing, and  $h$ ,  $k$ , and  $l$  are miller indices. The calculated lattice constants and spaces, and the shift of the (111) Bragg's peak of  $\text{Cd}_x\text{Zn}_{1-x}\text{Te}$  nanowire are presented in Table S1 and Fig. S3.† When the Cd percentage in the alloy increases, the lattice spacing increases (Fig. 1b) following the substitution of the Zn lattice by larger Cd atoms. An increase in the Cd amount increases the lattice constant as well and also the crystal structure becomes distorted. In both cases, the results are very close to the parameters for the corresponding thin films.<sup>18,19</sup> Vegard's law postulates a linear relation between the lattice parameters and the composition  $x$  for a continuous substitutional solid solution as:  $\alpha = x\alpha_{\text{CdTe}} + \alpha_{\text{ZnTe}}(1 - x)$  where  $\alpha_{\text{CdTe}}$ ,  $\alpha_{\text{ZnTe}}$ , and  $\alpha$  are the lattice parameters of CdTe, ZnTe, and  $\text{Cd}_x\text{Zn}_{1-x}\text{Te}$  respectively. By using this relation and applying the lattice parameters obtained from the XRD results, the amount of Cd in each composition was predicted and the chemical formula for each sample was obtained. The results compare well with the ones extracted from the EDX data at several segments of different nanowires from each sample (Table S2, ESI†). The results indicate the possibility of synthesizing alloy  $\text{Cd}_x\text{Zn}_{1-x}\text{Te}$  ( $0 \leq x \leq 1$ ) nanowires with modulated composition by accurate temperature control of the substrates.

The Raman spectra in Fig. 2 show four peaks for ZnTe nanowires at 204.5, 410.5, 616, and 820  $\text{cm}^{-1}$  which are related to the first, second, third, and fourth order longitudinal optical (LO) phonon scattering of ZnTe. Three peaks are seen at 140, 160, and 328  $\text{cm}^{-1}$  for CdTe nanowires. The first peak, 140  $\text{cm}^{-1}$ , is due to the transverse optical (TO) mode of CdTe while the second one, 160  $\text{cm}^{-1}$ , is assigned to the LO mode of CdTe nanowires and the peak at 328  $\text{cm}^{-1}$  is its second harmonic.<sup>20</sup> Even a small addition of Cd, for example  $\text{Cd}_{0.03}\text{Zn}_{0.97}\text{Te}$ , results in ZnTe peaks shifting slightly to the left at the lower frequency region and becoming weaker in comparison with pure ZnTe peaks. When the Cd fraction increases, the ZnTe peaks disappear and CdTe peaks appear strongly. This trend continues in the whole range of  $x$ . In a sample of  $\text{Cd}_{0.41}\text{Zn}_{0.59}\text{Te}$ , the peaks can be seen at 121, 148, 191, and 383  $\text{cm}^{-1}$ . The peak at 121  $\text{cm}^{-1}$  is likely due to Te aggregation, possibly arising from the E1

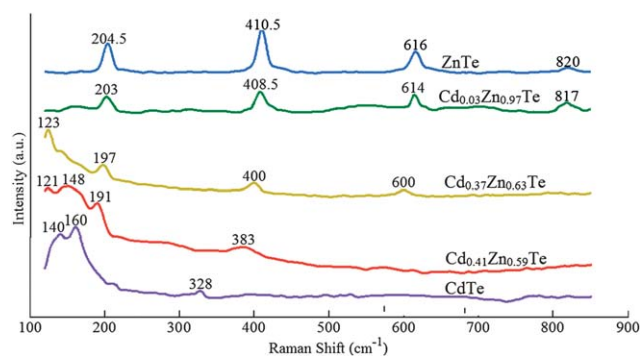


Fig. 2 Raman spectra of nanowires with different compositions.

symmetry of the phonon vibrations in the TeO structures.<sup>21</sup> The peak at 148  $\text{cm}^{-1}$  is related to the TO mode of CdTe and the peaks at 191 and 383  $\text{cm}^{-1}$  are assigned to the first and second order ZnTe LO phonon modes respectively.

The PL spectra (Fig. 3) were obtained from a pile of as-grown nanowires on a glass substrate rather than single nanowires on a silicon substrate, since individual nanowires had weak radiation intensity and a low PL yield. A pile of ZnTe NWs shows a single near-bandgap peak and narrow spectra (FWHM = 13 nm) which is due to the homogeneous composition of pure ZnTe nanowires.<sup>22</sup> The PL patterns become broader with increasing fraction of Cd in the alloy nanowires. A shift to lower energy emissions occurs gradually with an increase in the Cd content from 2.24 eV for pure ZnTe to 1.58 eV for  $\text{Cd}_{0.67}\text{Zn}_{0.33}\text{Te}$ . The estimated bandgaps from the measured PL spectra as a function of Cd composition determined from the XRD results are

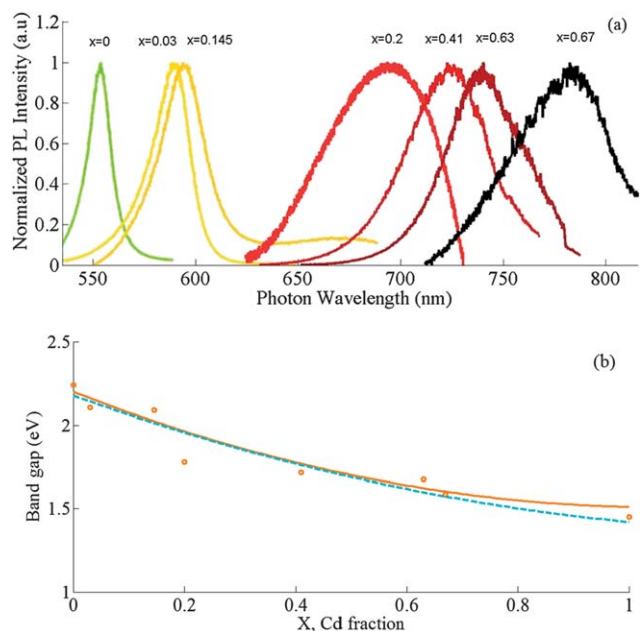


Fig. 3 (a) Normalized PL spectra obtained from  $\text{Cd}_x\text{Zn}_{1-x}\text{Te}$  nanowires for various values of  $x$ , with the excitation wavelength of 532 nm, and (b) estimated bandgaps of different alloy nanowires from PL spectra as a function of Cd fraction  $x$ . The best quadratic curve fitted to our experimental data (solid line), and the data for alloy thin films from ref. 23 are shown.

shown in Fig. 3b. The observed trend can be fitted to a quadratic relation:

$$\text{BG}(\text{Cd}_x\text{Zn}_{1-x}\text{Te}) = \text{BG}(\text{ZnTe}) + [\text{BG}(\text{CdTe}) - \text{BG}(\text{ZnTe}) - b]x + bx^2$$

where the coefficient  $b$  is known as the bowing parameter estimated as 0.61 from the least square fit of the data. The results here compare well with the bandgaps for the  $\text{Cd}_x\text{Zn}_{1-x}\text{Te}$  thin films.<sup>23</sup>

## 4 Conclusions

In summary,  $\text{Cd}_x\text{Zn}_{1-x}\text{Te}$  ( $0 \leq x \leq 1$ ) nanowires were synthesized using a vapor–liquid–solid method, and the alloy composition and thus the bandgaps were modulated through control of the substrate temperature. The difference in vapor pressures of the two telluride sources requires judicious mixing of the source powders and placement of the source boats inside the VLS furnace. The nanowires were stoichiometric and highly crystalline without any stacking faults or other defects. The results show that the energy gap modulation of single nanowires is possible in the range of visible to near infrared wavelengths.

## Acknowledgements

This work was supported by the World Class University program through the National Research Foundation of Korea funded by the Ministry of Education, Science and Technology under Project R31-2008-000-10100-0 and Postech National Center for Nanomaterials Technology (NCNT). SunHye Kim (RIST), Minhyeok Son (POSTECH Dept. of Chemistry) and Viktor Unterberger (TU Graz-Austria) are acknowledged for their help with characterization. This work was also partly supported by a grant (Code No. 2011-0031638) from the Center for Advanced Soft Electronics under the Global Frontier Research Program of the Ministry of Education, Science and Technology. GC and JP gratefully acknowledge support from the German Excellence Initiative via the Cluster of Excellence EXC 1056 “Center for Advancing Electronics Dresden” (cFAED).

## References

- 1 M. Meyyappan and M. K. Sunkara, *Inorganic Nanowires: Applications, Properties and Characterization*, CRC Press, Boca Raton, FL, 2010.
- 2 K. Wang, J. Chen, W. Zhou, Y. Zhang, Y. Yan, J. Pern and A. Mascarenhas, *Adv. Mater.*, 2008, **20**, 3248.
- 3 M. Law, L. E. Greene, A. Radenovic, T. Kuykendall, J. Liphardt and P. Yang, *J. Phys. Chem. B*, 2006, **110**, 22652.
- 4 W. Lu, J. Xiang, B. P. Timko, Y. Wu and C. M. Lieber, *Proc. Natl. Acad. Sci. U. S. A.*, 2005, **102**, 10046.
- 5 A. P. Pan, W. C. Zhou, E. S. P. Leong, R. B. Liu, A. H. Chin, B. S. Zhou and C. Z. Ning, *Nano Lett.*, 2009, **9**, 784.
- 6 J. A. Zapien, Y. K. Liu, Y. Y. Shan, H. Tang, C. S. Lee and S. T. Lee, *Appl. Phys. Lett.*, 2007, **90**, 213114.
- 7 Y. Liu, J. A. Zapien, Y. Y. Shan, C. Y. Geng, C. S. Lee and S. T. Lee, *Adv. Mater.*, 2005, **17**, 1372.
- 8 Y. K. Liu, J. A. Zapien, Y. Y. Shan, H. Tang, C. S. Lee and S. T. Lee, *Nanotechnology*, 2007, **18**, 365606.
- 9 X. Zhuang, C. Z. Ning and A. L. Pan, *Adv. Mater.*, 2012, **24**, 13.
- 10 F. X. Gu, Z. Y. Yang, H. K. Yu, P. Wang, L. M. Tong and A. L. Pan, *J. Am. Chem. Soc.*, 2011, **133**, 2037.
- 11 C. J. Kim, H. S. Lee, Y. J. Yang, R. R. Lee, J. K. Lee and M. H. Jo, *Adv. Mater.*, 2011, **23**, 1025.
- 12 J. E. Yang, W. H. Park, C. J. Kim, Z. H. Kim and M. H. Jo, *Appl. Phys. Lett.*, 2008, **92**, 263111.
- 13 K. Davami, D. Kang, J. S. Lee and M. Meyyappan, *Chem. Phys. Lett.*, 2011, **504**, 62.
- 14 K. Davami, H. M. Ghassemi, X. H. Sun, R. S. Yasser, J. S. Lee and M. Meyyappan, *Nanotechnology*, 2011, **22**, 435204.
- 15 J. F. Butler, F. P. Doty, B. Aptovsky, J. Lazerowicz and L. Verger, *Mater. Sci. Eng., B*, 1993, **16**, 291.
- 16 Y. Aisen and A. Shor, *J. Cryst. Growth*, 1998, **184/185**, 1302.
- 17 H. Heo, K. Kang, D. Lee, L. H. Jin, H. J. Back, I. Hwang, M. Kim, H. S. Lee, B. J. Lee, G. C. Yi, Y. H. Cho and M. H. Jo, *Nano Lett.*, 2012, **12**, 855.
- 18 S. Stolyarova, F. Edelman, A. Chack, A. Berner, P. Werner, N. Zakharov, M. Vytrykhivsky, R. Beserman, R. Weil and Y. Nemirovsky, *J. Phys. D: Appl. Phys.*, 2008, **41**, 065402.
- 19 K. P. Rao, O. Md. Hussain, K. T. R. Reddy, P. S. Reddy, S. Uthanna, B. S. Naidu and P. J. Reddy, *J. Alloys Compd.*, 1995, **218**, 86.
- 20 J. H. Ruelas, M. Lopez and O. Z. Angel, *J. Appl. Phys.*, 2000, **39**, 1701.
- 21 K. Prabakar, S. Venkatachalam, Y. L. Jeyachandran, Sa. K. Narayandass and D. Mangalaraj, *Mater. Sci. Eng., B*, 2004, **107**, 99.
- 22 M. Wang, G. T. Fei, Y. G. Zhang, M. G. Kong and L. D. Zhang, *Adv. Mater.*, 2007, **19**, 4491.
- 23 J. L. Reno and E. D. Jones, *Phys. Rev. B: Condens. Matter Mater. Phys.*, 1991, **45**, 1440.